

## Hall mobility of electrons in quantized accumulation layers on ZnO surfaces

Y. Grinshpan, M. Nitzan, and Y. Goldstein

Racah Institute of Physics, The Hebrew University of Jerusalem, 91000 Israel

(Received 3 October 1977)

Hall-effect measurements were performed on the (0001) face of ZnO single crystals under extreme accumulation layer conditions with surface electron densities ranging from  $\sim 10^{12}$  up to  $\sim 10^{14}$   $\text{cm}^{-2}$ . The measurements were performed as a function of the surface-electron density and temperatures in the temperature range of 2–300 K. The electron density in the accumulation layer was found to be essentially temperature independent over the whole temperature range. The electron mobility, on the other hand, is temperature dependent for surface-electron densities up to  $\sim 10^{13}$   $\text{cm}^{-2}$ , decreases with decreasing temperatures and at low temperatures carrier localization occurs. As a function of the surface-electron density (at a fixed temperature) the mobility initially increases, reaches a maximum, and then slowly decreases. The results suggest scattering and/or localization by charged scattering centers which apparently conglomerate into large clusters.

### I. INTRODUCTION

Considerable effort has been devoted in recent years to the study of quantization effects in narrow surface channels of semiconductors.<sup>1-3</sup> Most of the theoretical and experimental work was carried out on Si inversion layers at the Si-SiO<sub>2</sub> interface. The measurements were usually made on MOS structures, where excess surface-charge densities  $\Delta N$  of up to about  $10^{13}$   $\text{cm}^{-2}$  are attainable. Transport properties in quantized surface layers have received particular attention.<sup>1-6</sup> In spite of many differences in detail some general features are common to most of the reported data. At a fixed temperature (mostly at low temperatures) the mobility  $\mu$  as a function of the surface carrier density  $\Delta N$  initially increases, reaches a maximum, and then decreases gradually.<sup>4,5,7-9</sup> As a function of the temperature  $T$ , the surface conductance  $\Delta\sigma$  increases exponentially with  $T$  at small  $\Delta N$  and low  $T$ , while for larger  $\Delta N$  it becomes temperature independent.<sup>10-12</sup> The lowest value of  $\Delta\sigma$  which is already temperature independent is called the "minimum metallic conductivity"  $\sigma_{\text{min}}$ .

The increase of the mobility with surface carrier density at low  $\Delta N$  was explained, by various models.<sup>4,6,9,13</sup> All these models assume essentially that the main scattering is due to charged scattering centers whose effectiveness decreases with increasing carrier energy and/or screening by the mobile charge. The temperature dependence has been explained by trapping at the centers,<sup>1,5</sup> Anderson transition,<sup>1,10,11,14,15</sup> and percolation.<sup>14,16</sup> The decrease of mobility at higher-surface concentrations is attributed to other scattering processes, such as surface roughness, surface phonons, and intraband and intervalley scattering.<sup>1,3,9,17,18</sup> It must be pointed out, how-

ever, that quantitatively the different models fit only a limited range of experimental data and give mostly a qualitative picture of the transport properties in quantized surface channels.

ZnO is of particular interest for studies of quantized surface layers because of the huge electron densities that can be obtained on its surface.<sup>19-25</sup> Relatively clean ZnO crystals are  $n$ -type semiconductors, with a bulk conductivity of a few mho/cm. The Hall mobility<sup>26</sup> of the electrons in the bulk is of the order of 150  $\text{cm}^2/\text{V}\cdot\text{sec}$  at room temperature, increases to about 1000  $\text{cm}^2/\text{V}\cdot\text{sec}$  at liquid-nitrogen temperature and decreases towards lower temperatures. Doping<sup>20</sup> by Li compensates the ZnO crystals and they become insulating (over  $\sim 10^8$   $\Omega\cdot\text{cm}$ ). The use of such insulating crystals enables direct measurements of the properties of the surface-accumulation layers, similar to Hall measurements in inversion layers (which are effectively insulated from the bulk). There are several methods for producing strong accumulation layers on free ZnO surfaces: (i) illuminating ZnO crystals in vacuum by band-gap light (photon energy above  $\sim 3.2$  eV)<sup>20-23</sup>; (ii) exposure to atomic hydrogen.<sup>19,20,24,27</sup> In both these methods a positively charged layer obtains, probably due to desorption of oxygen<sup>20-22</sup> or CO<sub>2</sub>,<sup>28</sup> which is compensated with the strong accumulation of free electrons at the surface; (iii) exposure to thermalized He<sup>+</sup> ions, produced in an electrical discharge in helium gas at atmospheric pressure<sup>29</sup>; (iv) heating ZnO crystals in vacuum to temperatures of about 600K.<sup>19,20,25</sup>; (v) electron bombardment.<sup>20</sup> The accumulation layer may be reduced in each of these methods by exposure of the surface to oxygen. With the above methods surface electron concentrations up to  $3 \times 10^{13}$ – $10^{14}$   $\text{cm}^{-2}$  may be obtained, depending on the specific method used. These surface-carrier concentra-

tions are about one order of magnitude larger than those obtainable on silicon inversion layers in MOS structures. Thus ZnO seems to be a natural choice to explore the high- $\Delta N$  region unattainable in MOS structures.

Various authors investigated the electronic conduction properties of ZnO single crystals in bulk<sup>26,30-34</sup> and in surface-accumulation layers.<sup>19-22,29,35-37</sup> Most of the work on ZnO surfaces was primarily concerned with the adsorption-desorption mechanism<sup>20,22,23</sup> and surface states.<sup>20</sup> Field-effect and photoconductivity measurements were also performed,<sup>21,24</sup> but these cannot supply sufficient data on integrated mobility and electron concentration. Moreover, these measurements were usually made on the prism faces only. Recently, Kohl and Heiland<sup>25</sup> performed Hall-effect measurements on cleaved polar surfaces of ZnO at liquid-nitrogen temperature. They explored the region of relatively low surface-electron concentrations ( $10^7$ – $10^{13}$  cm<sup>-2</sup>) obtained by desorption.

In this paper we present detailed results of conductivity, Hall mobility, and surface-electron concentration. The measurements were performed over a wide range of surface electron densities  $\Delta N$  (up to  $\sim 10^{14}$  cm<sup>-2</sup>) and temperatures (1.6–300 K). We find that at relatively low  $\Delta N$  values ( $\sim 10^{13}$  cm<sup>-2</sup>) the mobility increases as a function of  $\Delta N$ , reaches a maximum at surface-electron densities of the order of  $5 \times 10^{13}$  cm<sup>-2</sup> and then decreases moderately at very high  $\Delta N$ . At low temperatures we observe carrier "localization" for low  $\Delta N$  values, but for high  $\Delta N$  values ( $\Delta N \geq 3 \times 10^{13}$  cm<sup>-2</sup>) there is no "localization" down to 1.6 K. The electron concentration is found to be essentially temperature independent over the entire temperature range.

The general behavior of the mobility in accumulation layers on ZnO is qualitatively similar to results obtained for quantized surface channels on other materials. There are, however, some significant differences which indicate the presence of charged scattering centers consisting of a large conglomeration of surface ions. Magnetoresistance measurements<sup>38</sup> also suggest the existence of such aggregation of surface ions.

## II. EXPERIMENTAL

Samples of ZnO single crystals were supplied by the Airtron Co. The samples were cut to typical dimensions of  $10 \times 2 \times 1$  mm<sup>3</sup>, with the hexagonal  $c$  axis perpendicular to the large surfaces. After lapping the polar (i.e., the large) surfaces, the samples were cleaned and etched in concentrated HCl. This etch enables one to distinguish between the (000 $\bar{1}$ ) oxygen face and the (0001) zinc

face.<sup>19</sup> Eight indium contacts were soldered to each sample, two of these on the end faces to serve as current contacts, the others were distributed on both sides, along the long dimension of the oxygen surface. All faces, excluding the investigated surface, namely, the oxygen (000 $\bar{1}$ ) face, were masked with Picein to prevent them from influencing the conductivity. The sample was mounted on a boron nitride substrate which provided a good thermal contact with, and electrical insulation from, the sample holder. A calibrated carbon resistor and a copper-constantan thermocouple were connected to the substrate, just underneath the crystal, for temperature measurements. The sample was then inserted into a cryogenic system where the temperature could be varied between 1.6 and 320 K. The temperature was controlled by a heater with a temperature stabilizer, and around 4.2 K by helium exchange gas. The magnetic field (up to  $\sim 3500$  G) was produced by a coil immersed in liquid nitrogen.

We have used two kinds of crystals: unintentionally doped crystals with room-temperature bulk resistivity of the order of  $10$   $\Omega$ -cm and insulating samples, compensated with Li, of bulk resistivity well over  $10^8$   $\Omega$ -cm. Two methods were used to produce high surface-electron densities: illumination of the crystal while in vacuum of about  $10^{-5}$  Torr, or exposure to He<sup>+</sup> ions. With the first method we could produce medium-strong accumulation layers of up to surface-electron densities of about  $4 \times 10^{13}$  cm<sup>-2</sup>. After the illumination the accumulation layer could be maintained for long periods by simply leaving it in vacuum. Letting dry oxygen into the system destroyed the accumulation layer gradually. With the second method (electrical discharge in helium) much higher surface-electron concentrations were obtained, up to  $(1-2) \times 10^{14}$  cm<sup>-2</sup>. Such high accumulation layers could be maintained for longer times generally only when cooled below  $\sim 100$  K. At higher temperatures these very strong accumulation layers usually slowly decayed, even at pressures of  $10^{-5}$  Torr. Admitting oxygen into the system at room temperature, caused a fast decrease in the accumulation layer.

Homogeneity and conductivity measurements were carried out by measuring the voltage drop along the crystals when passing current derived from a constant-current source between the end contacts. At relatively low surface-carrier densities, the current contacts became increasingly noisy at low temperatures, and this set the limit to our measurements. The Hall effect was usually measured between three pairs of parallel probes (the Hall probes). We considered only those results where the differences between the pairs

were less than 10%. In the insulating crystals the Hall effect and conductivity yield directly the surface Hall mobility  $\mu_H$  and Hall constant. The Hall constant  $R_H'$  for surface channels is usually defined as  $R_H' = E_H/IB$ , using the value of the current  $I$  instead of the current density  $J$ . (Here  $E_H$  is the Hall field and  $B$  the magnetic induction.) Since in the accumulation layer only electrons are present we can interpret<sup>39</sup> the Hall constant as  $R_H' = 1/e\Delta N$ , where  $e$  is the absolute value of the electronic charge and  $\Delta N$  the surface-electron density. In the conducting samples, Hall measurements yield some combination of surface and bulk parameters,<sup>39</sup> so that information from these crystals was extracted for two limiting cases only: (a) before any surface treatment. In this case the measurements in dark yield the bulk values of the electron density  $n_b$  and mobility  $\mu_b$ ; and (b) with a strong accumulation layer and at low temperatures where the bulk carriers are essentially "frozen out" and the samples become insulating.

The following measurement procedure was usually employed: A strong accumulation layer was produced by one of the methods mentioned above. The sample was then gradually cooled down, and measurements were taken at prefixed temperature intervals. After reaching the lowest temperature the sample was again heated to room temperature and the conductivity was monitored as a function of the temperature and checked against previous measurements. This was done to ensure that no conductivity decay occurred during the cycle due to oxygen adsorption. The results agreed usually within 1%–2%, so that in every cycle the surface remained in the same condition. At room temperature some oxygen was then let into the system and after the desired reduction in the conductivity had been obtained the system was again evacuated and the cycle repeated in the new surface condition.

### III. RESULTS

Hall-effect measurements were performed on a variety of samples, in all of which the surface studied was the oxygen face (000 $\bar{1}$ ). We found that there are appreciable variations between the results for different samples, although the procedure of surface preparation was the same. We believe that these variations are inherent in the disordered nature of the surface. Yet a general trend and behavior of the transport properties is apparent from the different measurements. This is demonstrated in Fig. 1, where we have plotted the room-temperature surface Hall mobility  $\mu_H$  as a function of the surface-electron density  $\Delta N$  for six samples. The accumulation layers were pro-

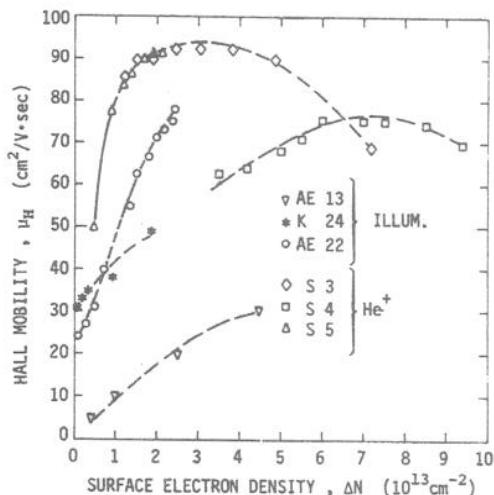


FIG. 1. Surface Hall mobility  $\mu_H$  as a function of surface-electron density at room temperature. Measurements are shown for various samples, for which the accumulation layer had been generated either by illumination or by exposure to  $\text{He}^+$  ions, as marked.

duced either by illumination or exposure to  $\text{He}^+$  ions, as marked in the figure. The range of surface-electron concentrations investigated was from a few times  $10^{11} \text{ cm}^{-2}$  to about  $10^{14} \text{ cm}^{-2}$ . We could not measure the mobility at lower densities because the surface became inhomogeneous and the results were unreliable. Also, at low densities the contact noise became too large. In spite of the large variation in the results some general characteristics are evident. At low surface-electron densities the mobility is relatively low and rises fairly fast with increasing  $\Delta N$ . For the accumulation layers produced by illumination the mobility increase persists up to the highest concentrations reached. On samples where accumulation layers were produced by exposure to  $\text{He}^+$  ions, the mobility reaches a maximum and then decreases with increasing  $\Delta N$ . This decrease is usually slower than the fast initial rise. As can be seen, the value of the surface-electron concentration where the maxima occur, varies from sample to sample. The rates of increase or decrease of  $\mu_H$  with  $\Delta N$  vary as well from sample to sample.

In Fig. 2 we plotted, on a log-log scale, typical results of the surface conductance  $\Delta\sigma$  as a function of the temperature  $T$ , for different surface conditions. Each curve corresponds to a temperature run as described in Sec. II. As we shall see below, during a temperature run the surface-electron density remained constant and thus we characterize the different curves by the corresponding value of  $\Delta N$ . Figure 2(a) shows the surface conductance of two samples in the temperature range

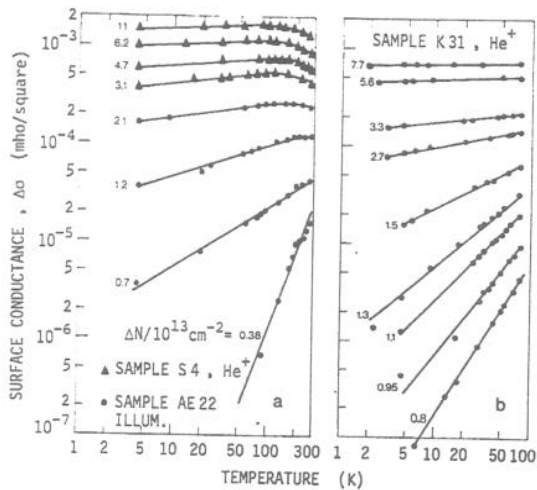


FIG. 2. Log-log plots of the surface conductance  $\Delta\sigma$  as a function of temperature, at several surface-electron concentrations  $\Delta N$ . (a) Results for relatively low surface-electron densities (prepared by illumination) and for very high surface-electron densities (prepared by exposure to  $\text{He}^+$  ions). (b)  $\Delta\sigma$  vs  $T$  for several surface-electron concentrations, from relatively low  $\Delta N$  up to very strong accumulation layers on the same sample, K31.

4.2–300 K and surface-electron densities in the range  $3.8 \times 10^{12}$ – $1.1 \times 10^{14}$   $\text{cm}^{-2}$ . The accumulation layers on the two samples were produced by the two different methods as noted in Fig. 2. Note that here the maximum surface-electron density reached was as high as  $1.1 \times 10^{14}$   $\text{cm}^{-2}$ . This was one of the few cases where the very strong accumulation layer did not decay even at room temperature. The surface conductance in strong accumulation layers (above  $(2-3) \times 10^{13}$   $\text{cm}^{-2}$ ) is almost independent of temperature. There is a slight increase in conductivity when the temperature increases from 4.2 to  $\sim 100$  K and then  $\Delta\sigma$  slightly decreases with a further increase in  $T$ . The value of the maximum seems to move to higher temperatures with decreasing surface-electron density. These changes are, however, quite small and on the whole we may consider the conductance at these high densities close to metallic. At lower concentrations, it is apparent that the conductivity is strongly dependent on the temperature and surface-electron density. At a given surface condition the conductivity decreases with decreasing temperatures; the lower  $\Delta N$  the stronger the temperature dependence. On the log-log plot of Fig. 2(a) the experimental points lie on straight lines whose slopes increase as  $\Delta N$  is reduced.

In Fig. 2(b) similar results are shown for a third sample (sample K31). The accumulation layer on this sample was produced by exposure to  $\text{He}^+$  ions, and the temperature could not be raised

much above 77 K since this caused a decay of the surface-electron concentration. We again see the metallic conductivity at high accumulation layers and the pronounced decrease of the conductivity with decreasing  $T$  for surface electron densities below  $\sim 3 \times 10^{13}$   $\text{cm}^{-2}$ . On the sample of Fig. 2(b) we performed also extensive magnetoresistance measurements. The results of these measurements are being reported elsewhere.<sup>38</sup>

In Fig. 3 we plot typical Hall-effect measurements of the accumulation-layer electron concentration  $\Delta N$  as a function of temperature. Here again each curve corresponds to a temperature run at fixed surface conditions. The temperature ranged from 2 to 300 K, and the surface-electron densities covered a range from  $5 \times 10^{12}$  to  $10^{14}$   $\text{cm}^{-2}$ . The interesting result is that  $\Delta N$  is independent of temperature for all densities measured. Apart from small variations which might be due to changes in the Hall factor  $r_H$  as a function of the temperature, and small irregularities at temperatures above 100 K, which differ from sample to sample,  $\Delta N$  remains on the whole constant down to the lowest temperatures measured. This is true also for lower surface densities (not shown in the figure) where, because of contact noise, we could not take measurements at temperatures below  $\sim 100$  K. These results mean that the strong temperature dependence of the conductivity shown in Fig. 2, is due to the temperature dependence of the mobility and not "freeze-out" effects of the surface electrons.

Figures 4 and 5 are log-log plots of the temperature dependence of the Hall mobility. Figure 4 shows typical results in the temperature range

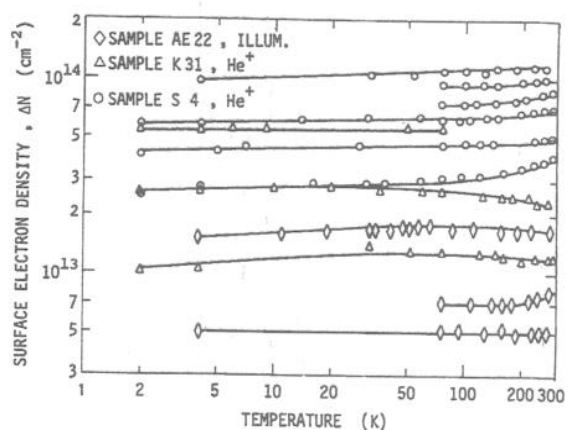


FIG. 3. Log-log plot of the surface-carrier density  $\Delta N$  as a function of temperature for different accumulation layers. Results are shown for three samples, both methods of preparation of accumulation layers were used.



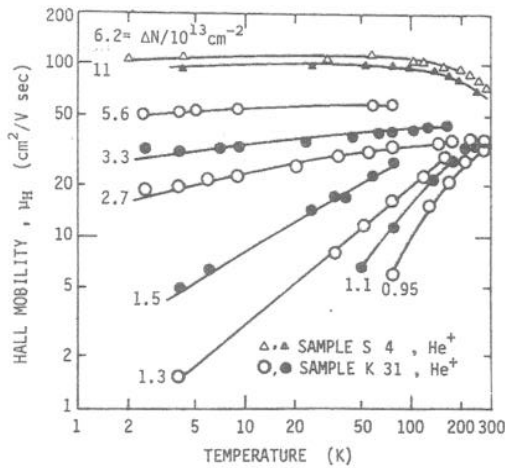


FIG. 4. Log-log plot of the surface Hall mobility as a function of temperature, at several surface-carrier densities. Results are shown for two samples, S4 and K31; the accumulation layer for both samples was produced by He<sup>+</sup> ions as indicated.

2–300 K for different values of  $\Delta N$  in strong and medium accumulation layers produced by exposure to He<sup>+</sup> ions (as noted in the figure). We see from these plots that the mobility is indeed almost independent of temperature at very strong accumulation layers, i.e., for  $\Delta N$  above  $\sim 3 \times 10^{13} \text{ cm}^{-2}$ . At lower surface-electron densities,  $\mu_H$  is tem-

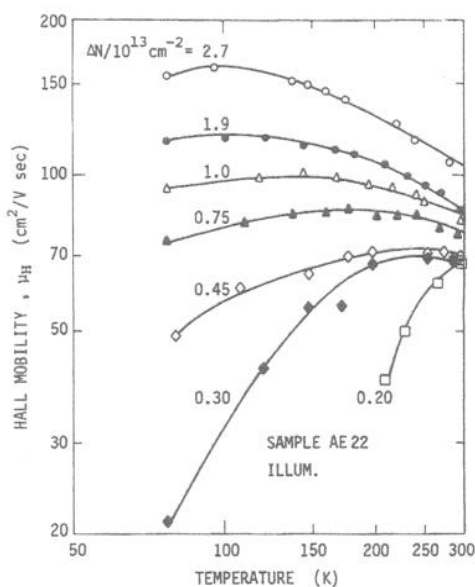


FIG. 5. Log-log plot of the surface Hall mobility as a function of temperature, at relatively low surface-electron densities. Each curve represents results for one value of  $\Delta N$ . The accumulation layer was produced by illumination, as marked.

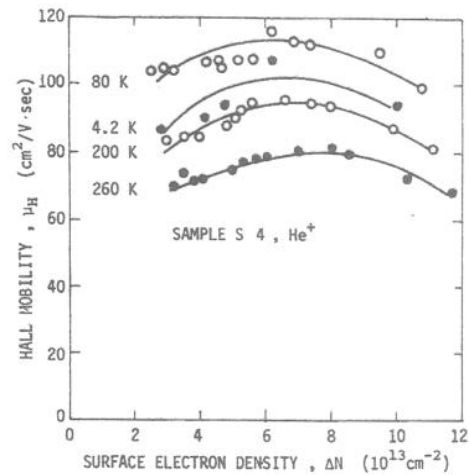


FIG. 6. Surface Hall mobility as a function of the surface-electron concentration at four temperatures, for very high surface-electron densities (prepared by exposure to He<sup>+</sup> ions).

perature dependent just as the conductivity is at the corresponding surface-electron densities (Fig. 2). We wish to point out that for the data at the very low values of the mobility (below  $\sim 5 \text{ cm}^2/\text{V sec}$ ) we were unable to measure the Hall effect because of the excessive contact noise at low conductances. These data were obtained by dividing the values of  $\Delta\sigma$  measured at the proper temperature by the values of  $\Delta N$  determined at higher temperatures. This seems to us legitimate in view of the fact that the surface-electron concentration is practically temperature independent. Figure 5 is a similar plot to Fig. 4 for the lower electron concentration ranges ( $2 \times 10^{12}$ – $2.7 \times 10^{13} \text{ cm}^{-2}$ ) produced by illumination. These measurements were taken in the temperature range of 77–300 K. We can see that at low surface densities, the mobility depends very strongly on the temperature. At low temperatures the mobility increases with increasing  $T$ , reaches a maximum and at not too low surface densities it decreases again with a further increase of  $T$ .

In Figs. 6–8, we present results of the Hall mobility  $\mu_H$  as a function of the surface-electron concentration  $\Delta N$ . Figure 6 shows results for strong accumulation layers obtained by the He<sup>+</sup>-deposition method. Here  $\mu_H$  is plotted as a function of  $\Delta N$  at four different temperatures. We see that the mobility depends only weakly on  $\Delta N$  at all temperatures. There is a small increase in  $\mu_H$  with  $\Delta N$  at the lower concentrations (up to  $\sim 7 \times 10^{13} \text{ cm}^{-2}$ ) and then a slight decrease, but the changes are at most of the order of  $\sim 15\%$ . The curves at the different temperatures, from as low as 4.2 up to

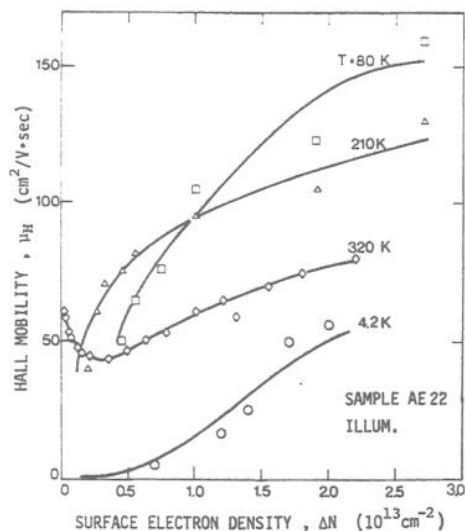


FIG. 7. Surface Hall mobility as a function of surface-electron density at four temperatures, at relatively low surface-electron densities (prepared by illumination).

260 K, are alike and the previously described behavior with  $T$  is again apparent.

Figure 7 presents results of  $\mu_H$  vs  $\Delta N$  for the range of relatively low-electron densities as obtained by illumination. Again we have plotted the results for a set of characteristic temperatures. At 4.2 K the mobility is very low and rises with increasing  $\Delta N$ . The same is true for the results at 80 and 210 K. The crossover of these curves stresses the fact that at higher temperatures the

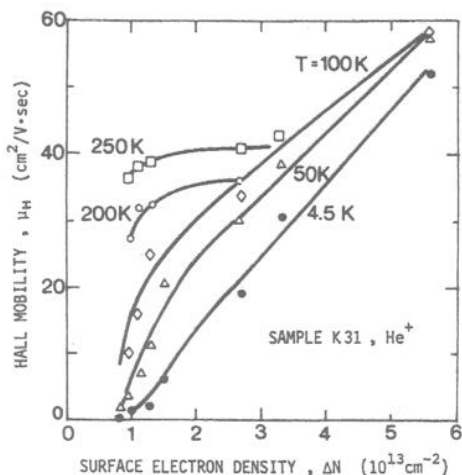


FIG. 8. Surface Hall mobility as a function of surface-electron density for a relatively low-mobility sample (K31, used also for magnetoresistance measurements).

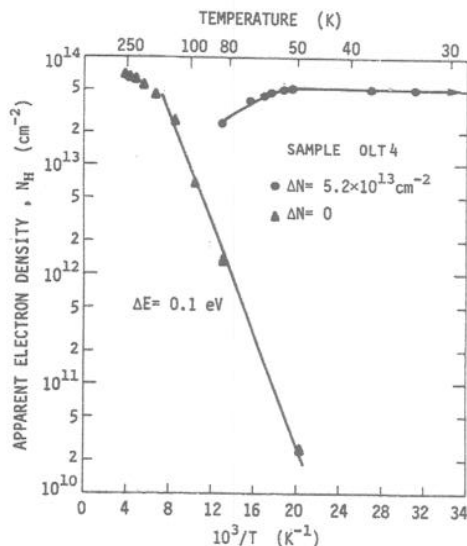


FIG. 9. Semilogarithmic plot of the apparent electron density  $N_H$  as a function of  $1/T$  on a conducting sample. The triangles represent the bulk values (before any surface treatment). The activation energy  $\Delta E$ , derived from the slope of the straight line, is marked in the figure. The dots show the results obtained when a strong accumulation layer with electron density  $\Delta N = 5.2 \times 10^{13}$  cm<sup>-2</sup> was present. The measurements were continued down to 4.2 K and a constant value for  $N_H$  was obtained as indicated by the arrow on the horizontal line.

mobility becomes less dependent on  $\Delta N$ . At 320 K the mobility is lower than at 80 and 210 K and is almost independent of  $\Delta N$ . It is interesting to note the decrease of the mobility with increasing  $\Delta N$  for the lowest values of the surface-electron densities. This may be an indication of the crossover between different mechanisms of surface scattering. Figure 8 is a plot of the Hall mobility as a function of surface-electron concentration for another sample (sample K31) starting at  $\Delta N \approx 10^{13}$  cm<sup>-2</sup> and going up to  $\approx 6 \times 10^{13}$  cm<sup>-2</sup>. In contrast to Fig. 6 we see here a pronounced increase with  $\mu_H$  with increasing  $\Delta N$  at low temperatures, which becomes more moderate at elevated temperatures.

In order to compare the transport properties at the surface and in the bulk, we performed measurements on semiconducting samples. First we measured the bulk mobility and bulk carrier density as a function of temperature, prior to any surface treatment and in the dark. Next the crystal was exposed to He<sup>+</sup> ions until a high accumulation layer was produced. We then measured once more the mobility and carrier concentration as a function of temperature. The results are shown in Figs. 9 and 10. In Fig. 9 we plotted on a semilog scale the apparent electron density per cm<sup>2</sup> as a function of  $1/T$  for the temperature range 30-

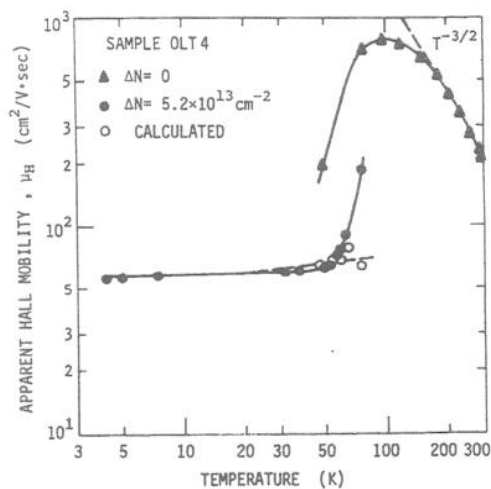


FIG. 10. Log-log plot of the apparent measured Hall mobility vs temperature, for the conducting sample of Fig. 9. The triangles represent bulk measurements, while the dots the measurements after producing the accumulation layer. The dotted line for bulk measurements represent the  $T^{-3/2}$  behavior of the bulk mobility. The empty circles are the calculated surface mobilities according to Eq. (1).

300 K. This density was calculated simply from the measured Hall factor  $R'_H$  as  $N_H = 1/eR'_H$ . The triangles represent results prior to the surface treatment, while the dots represent results obtained after producing a strong accumulation layer. Since this accumulation layer did not persist at temperatures above 77 K the measurements were taken only below liquid-nitrogen temperatures. For the "bulk" measurements we obtained the well-known<sup>31-34</sup> behavior of bulk electrons in ZnO. The carrier density increases exponentially with increasing temperatures with an activation energy of  $\sim 0.1$  eV, and tends to saturate at room temperature where the donors become almost completely ionized. It is important to note that at temperatures below 50 K the bulk carriers are essentially frozen out. After producing the accumulation layer the behavior of the apparent carrier concentration  $N_H$  changed completely. At very low temperatures (below 50 K) it was completely temperature independent to the lowest temperature measured (4.2 K, not shown in the figure). Between 50 and 77 K,  $N_H$  decreases with increasing  $T$ . In similar measurements, not shown here, we observed the same decrease, then a minimum, and at temperatures above  $\sim 100$  K, the  $N_H$  curves for both cases (before and after surface treatment) coincided. In Fig. 10 we plot, on a logarithmic scale, the dependence of the apparent mobility on temperature for the same measurements. For the "bulk" measurements we again observe the typical<sup>31-34</sup> behav-

ior of electron mobility in bulk ZnO. The mobility increases from the usual room temperature value of  $\sim 200$  cm<sup>2</sup>/V sec to about 800 cm<sup>2</sup>/V sec at 100 K, following approximately a  $T^{-3/2}$  law, and then decreases with decreasing temperatures. The measurements had to be discontinued at  $\sim 50$  K because of contact noise. In contrast, the mobility with an accumulation layer on the surface is constant at temperatures below 50 K, increasing with  $T$  at higher temperatures, but remaining lower than the former "bulk" value. Measurements at higher temperatures carried out on another sample showed that above 100 K the mobility curves coincided.

If we adapt the simple picture of the accumulation-layer conductivity being parallel to that of the bulk conductivity we obtain<sup>39</sup> the relation

$$N_H = (N_b \mu_b + \Delta N \mu_s)^2 / (N_b \mu_b^2 + \Delta N \mu_s^2), \quad (1)$$

where  $N_b \equiv n_b d$  is the bulk electron density per cm<sup>2</sup> of the surface,  $\mu_b$  is the bulk mobility,  $\mu_s$  the mobility of the accumulation-layer electrons, and  $d$  is the thickness of the sample. Using the values of  $N_b(T)$  and  $\mu_b(T)$  as obtained from the bulk measurements, and of  $\Delta N$  as obtained from the low-temperature measurements of  $N_H$  ( $\Delta N \approx 5.2 \times 10^{13}$  cm<sup>-2</sup>) we calculated the values of the surface mobility as a function of the temperature. A few such points are shown by empty circles in Fig. 10. We see that after the correction the surface mobility is temperature independent, just as expected at this high surface-electron density.

#### IV. DISCUSSION

In Sec. III we presented detailed results on conductivity and Hall effect in very strong accumulation layers on the ZnO (000 $\bar{1}$ ) face. The measurements were performed at the temperature range of 2–300 K and surface-carrier concentrations from  $\sim 2 \times 10^{11}$  cm<sup>-2</sup> to  $1.2 \times 10^{14}$  cm<sup>-2</sup>. The extremely high densities of  $10^{14}$  cm<sup>-2</sup> have not been obtained yet on any semiconductor. We found an appreciable quantitative variation in results from sample to sample but the overall, qualitative behavior is similar. The gross features of our results can be summarized as follows. At a fixed temperature,  $\mu_H$  increases with  $\Delta N$  at low  $\Delta N$ , reaches a maximum and then slowly decreases with  $\Delta N$  at very high  $\Delta N$ . The value of  $\Delta N$  for a given state of the surface was found to be temperature independent down to the lowest values of  $\Delta N$  and temperatures measured. Thus there is no "carrier freeze out." The mobility, on the other hand, and thus the surface conductance as well, are temperature independent only at relatively high surface-electron concentrations, above

$\sim 3 \times 10^{13} \text{ cm}^{-2}$ . At lower surface-electron densities  $\mu_H$  and  $\Delta\sigma$  become temperature dependent, decreasing with decreasing temperature and at low temperatures the electrons become localized. The temperature dependence becomes stronger the lower  $\Delta N$  is. Our results can be best fitted by the relation  $\Delta\sigma \propto T^\gamma$ , where  $\gamma$  ranges from zero at high  $\Delta N$  to  $\gamma \approx 2.5$  at  $\Delta N \approx 3.8 \times 10^{12} \text{ cm}^{-2}$ . The value of  $\sigma_{\text{min}}$ , the minimum metallic conductivity, is of the order of  $10^{-4}$  mho/square.

As already mentioned above, a behavior somewhat similar to ours has been observed<sup>10-12</sup> also on silicon inversion layers at low temperatures. Pepper *et al.*<sup>10</sup> found that the minimum metallic conductivity  $\sigma_{\text{min}}$  was of the order of  $10^{-5}$  mho/square, i.e., one order of magnitude lower than ours. Licciardello and Thouless<sup>40</sup> derived theoretically a universal value of  $3 \times 10^{-5}$  mho/square for two-dimensional systems. Hartstein and Fowler,<sup>12</sup> on the other hand, have shown on Si MOS structures that  $\sigma_{\text{min}}$  is a function of the ionic charges in  $\text{SiO}_2$ . The larger the charge density the smaller becomes  $\sigma_{\text{min}}$ . This was attributed to the increasing overlap between the scattering centers as the average distance between them decreases. For an ionic density of about  $10^{12} \text{ cm}^{-2}$  the above authors observed a minimum metallic conductivity of  $\sim 10^{-4}$  mho/square, the same order of magnitude as ours. The detailed temperature dependence as observed<sup>10-12</sup> on Si inversion layers, however, differs somewhat from ours and can be best fitted to the relation  $\Delta\sigma \propto e^{-\alpha/T^\beta}$ , where  $\beta$  is either 1 or  $\frac{1}{2}$ , depending on the temperature range. Another point of difference is that the position of the maximum in the  $\mu$  vs  $\Delta N$  curve for the ZnO channels occurs at values of  $\Delta N$  about one order of magnitude higher than in silicon channels.

The simplest feature of the data is the gradual decrease of the mobility with  $\Delta N$  at high values of  $\Delta N$ . This can be explained, as in the case of silicon, by the classical theories<sup>9,39,41,42</sup> of surface scattering. Even though at these concentrations the electrons become a quasi-two-dimensional gas, we can still expect a decreasing mobility with increasing  $\Delta N$ . This is because of the decrease in the effective width of the accumulation layer and thus an increased scattering due to surface roughness, phonons, and intraband and inter-valley scattering.<sup>1,3,9,17,18</sup>

The rise of the mobility with increasing  $\Delta N$  at low  $\Delta N$ , however, points clearly to a charged-centers scattering mechanism.<sup>4,6,9,13</sup> At the same time, the appreciable temperature dependence observed for low  $\Delta N$  (at low temperatures) indicates also the presence of some kind of a localization mechanism.<sup>1,6,10,11,14-16</sup> Increasing  $\Delta N$  and/or  $T$ , reduces such localization. For  $\Delta N$

above  $\sim 3 \times 10^{13} \text{ cm}^{-2}$ , where "metallic conductivity" obtains, further increase of  $\Delta N$  results in reduced scattering (increasing mobility) due probably to increasing screening of the charged scatterers.

The important question that now arises is the origin of the charged scattering centers. It seems natural to associate the ionic charge in the scattering centers with the positive surface charge (for example, excess  $\text{Zn}^+$ ) required to neutralize the negative space charge of the accumulation layer. This would imply a concentration of scattering centers of the order of  $\Delta N$  ( $\sim 10^{13} \text{ cm}^{-2}$ ). On the other hand, the value of the minimum metallic conductivity on ZnO surfaces indicates, analogously to the case of silicon,<sup>12</sup> a much lower concentration of scattering centers ( $\sim 10^{12} \text{ cm}^{-2}$ ). This dilemma can be resolved by assuming that the positive charge on the surface conglomerates into large clusters. The potential wells due to such clusters would be relatively deep, and because of the lower cluster density the overlap between them would be small. This hypothesis can also explain why the electrons in ZnO surface channels become delocalized only at relatively high values of  $\Delta N$ . The clusters would also constitute very efficient charged scattering centers and can thus explain the position of the mobility maxima (as a function of  $\Delta N$ ) in ZnO with respect to their position in Si. The larger the cluster, the more efficient the scattering, and only at very high  $\Delta N$  is the screening sufficiently large for surface roughness to dominate the scattering. Such charged clusters were already found experimentally by Di Stefano<sup>43</sup> and by Williams and Woods<sup>44</sup> at the Si-SiO<sub>2</sub> interface, and interpreted<sup>45</sup> as due to image forces. Magnetoresistance measurements<sup>38</sup> on ZnO surfaces carried out in this laboratory are also consistent with the clustering model. The functional dependence of the negative magnetoresistance found indicates the presence at the surface of scattering centers with giant magnetic moments of the order of  $100\mu_B$  (where  $\mu_B$  is the Bohr magneton).

Results of measurements on conducting samples, presented above, show that the existence of the accumulation layer is revealed by Hall-effect measurements only at low temperatures. Below  $\sim 50$  K when the bulk carriers freeze out one obtains the usual temperature independent surface mobility and  $\Delta N$ . From these measurements we conclude that the accumulation-layer conductivity does not depend on the nature of the crystal bulk (conducting or insulating). It is interesting to note also that assuming that  $\mu_H$  and  $\Delta N$  of the accumulation layer on the conducting samples remain approximately constant up to room temperature, we find that for  $T = 300$  K,  $\mu_b$  is approximately four



times as large as the surface mobility. (Such measurements of bulk mobility cannot be carried out on insulating samples.) This is quite natural in view of the additional scattering the surface electrons suffer.

Kohl and Heiland<sup>25</sup> measured the Hall mobility on the oxygen face of cleaved ZnO crystals at 90 K. At very low surface densities ( $2 \times 10^7$ – $10^{10}$  cm<sup>-2</sup>) these authors found an oscillating surface mobility with values ranging from about 600 to 1700 cm<sup>2</sup>/V sec. At higher surface densities and especially in the range of  $10^{12}$ – $10^{13}$  cm<sup>-2</sup>, which is of main interest in context with the present work, they observed an almost  $\Delta N$ -independent surface mobility of the order of 50–100 cm<sup>2</sup>/V sec, which slightly tends to decrease with increasing surface electron concentration. The above range of surface densities corresponds to the lowest  $\Delta N$  we could measure at that temperature and where we observed a very pronounced increase of  $\mu$  with  $\Delta N$ . Since there is only a limited amount of data for this range of surface densities in Kohl and Heiland's work, it is difficult to explain this difference; it might originate from the different pre-treatments of surfaces. Previous measurements by Heiland *et al.*<sup>19,20</sup> and by Krusemeyer<sup>21</sup> on ZnO prism surfaces indicate an increasing *field-effect mobility* with increasing  $\Delta\sigma$  at low surface conductivities, in agreement with results obtained in our laboratory on the polar surfaces.

Hausmann and Teuerle<sup>32</sup> reported "peculiar" results of mobility on ZnO conducting samples. In the course of their work on ZnO bulk mobility, they obtained curves very similar to those in Figs. 9 and 10. Prior to their measurements,

Hausmann and Teuerle<sup>32</sup> heated their ZnO samples to 1500 K in vacuum. They interpreted the results as being due to new shallow donors in the bulk. The authors also observed negative magnetoresistance for these samples at low temperatures. Measurements on ZnO samples in our laboratory revealed an increase of the conductivity due to heating the crystals in vacuum. This increased conductivity disappears, at least partially, by letting oxygen into the system. We therefore believe that Hausmann and Teuerle<sup>32</sup> had unknowingly a very strong accumulation layer on their samples which caused their "peculiar" behavior.

In conclusion, we have investigated the transport properties of very strong accumulation layers on ZnO. Our mobility results suggest that the dominant scattering mechanism at the surface is due to scattering and/or localizing centers, consisting probably of large aggregates of positive charges. At low surface densities and low temperatures, the electrons become localized. By increasing the surface density  $\Delta N$  the mobility increases due to partial screening of the scattering center's charge. Increasing  $\Delta N$ , as well as raising the temperature, causes the electrons to be delocalized and thus also enhances their mobility.

#### ACKNOWLEDGMENTS

We wish to thank A. Many for many helpful suggestions and critical discussions. This work was supported by a grant from the National Council for Research and Development, Israel and the KFK (Kernforschungszentrum Karlsruhe GmbH), Germany.

<sup>1</sup>F. Stern, *Crit. Rev. Solid State Sci.* **4**, 499 (1974).

<sup>2</sup>G. Dorda, in *Advances in Solid State Physics XIII*, edited by H. J. Queisser (Pergamon-Vieweg, New York, 1973), p. 215.

<sup>3</sup>T. Sugano, K. Hoh, H. Sakaki, T. Iizuka, K. Hirai, K. Kuroiwa, and K. Kakemoto, *J. Fac. Eng., Univ. Tokyo B* **32**, 159 (1973).

<sup>4</sup>S. Kawaji and Y. Kawaguchi, *J. Phys. Soc. Jpn.* **21**, 337 (1966).

<sup>5</sup>F. F. Fang and A. B. Fowler, *Phys. Rev.* **169**, 619 (1968).

<sup>6</sup>F. Stern and W. E. Howard, *Phys. Rev.* **163**, 816 (1967).

<sup>7</sup>T. Sugano, H. Sakaki, and K. Hoh, *J. Jpn. Soc. Appl. Phys.* **39**, 192 (1970).

<sup>8</sup>A. Toscano-Rico and J. C. Pfister, *Phys. Status Solidi A* **15**, 209 (1971).

<sup>9</sup>Y. C. Cheng, *J. Appl. Phys.* **44**, 2425 (1973); Y. C. Cheng and S. E. Sullivan, *ibid.* **44**, 923 (1973).

<sup>10</sup>M. Pepper, S. Pollitt, C. J. Adkins, and R. A. Stradling, *Crit. Rev. Solid State Sci.* **5**, 375 (1975); M. Pepper, S. Pollitt, C. J. Adkins, and R. E. Oakley, *Phys. Lett. A* **47**, 71 (1974); **47**, 113 (1974).

<sup>11</sup>S. Pollitt, M. Pepper, and C. J. Adkins, *Surf. Sci.* **58**, 79 (1976).

<sup>12</sup>A. Hartstein and A. B. Fowler, *J. Phys. C* **8**, L249 (1975).

<sup>13</sup>F. Berz, *Solid State Electron.* **13**, 903 (1970).

<sup>14</sup>E. Arnold, *Surf. Sci.* **58**, 60 (1976).

<sup>15</sup>F. Stern, *Phys. Rev. B* **9**, 2762 (1974); *J. Vac. Sci. Technol.* **11**, 962 (1974).

<sup>16</sup>E. Arnold, *Appl. Phys. Lett.* **25**, 705 (1974).

<sup>17</sup>R. F. Greene, *Crit. Rev. Solid State Sci.* **5**, 345 (1975).

<sup>18</sup>D. K. Ferry, in *Proceedings of the 13th International Conference on the Physics of Semiconductors, Rome, 1976*, edited by F. G. Fumi (Marves, Rome, 1977), p. 758.

<sup>19</sup>G. Heiland and P. Kunstmann, *Surf. Sci.* **13**, 72 (1969).

<sup>20</sup>G. Heiland, E. Mollwo, and F. Stöckmann, *Solid State Phys.* **8**, 193 (1958).

<sup>21</sup>H. J. Krusemeyer, *Phys. Rev.* **114**, 655 (1959); *J. Phys. Chem. Solids*, **23**, 767 (1962).

<sup>22</sup>A. Many, *Crit. Rev. Solid State Sci.* **4**, 515 (1974).

<sup>23</sup>D. Eger, Y. Goldstein, and A. Many, *RCA Rev.* **36**,

- 508 (1975).
- <sup>24</sup>G. Heiland, *J. Phys. Chem. Solids* **6**, 155 (1958).
- <sup>25</sup>D. Kohl and G. Heiland, *Surf. Sci.* **63**, 96 (1977).
- <sup>26</sup>A. R. Hutson, *J. Phys. Chem. Solids* **8**, 467 (1959).
- <sup>27</sup>Y. Shapira and D. Lichtman, *J. Vac. Sci. Technol.* **13**, 615 (1976).
- <sup>28</sup>Y. Shapira, S. M. Cox, and D. Lichtman, *Surf. Sci.* **54**, 43 (1976).
- <sup>29</sup>Y. Goldstein, A. Many, D. Eger, Y. Grinshpan, G. Yaron, and M. Nitzan, *Phys. Lett. A* **62**, 57 (1977).
- <sup>30</sup>A. R. Hutson, *Phys. Rev.* **108**, 222 (1957).
- <sup>31</sup>P. Wagner and R. Helbig, *J. Phys. Chem. Solids*, **35**, 327 (1974).
- <sup>32</sup>A. Hausmann, and W. Teuerle, *Z. Phys.* **259**, 189 (1973).
- <sup>33</sup>B. Utsch and A. Hausmann, *Z. Phys. B* **21**, 27 (1975).
- <sup>34</sup>A. Hausmann and B. Utsch, *Z. Phys. B* **21**, 217 (1975).
- <sup>35</sup>G. Heiland, *Faraday Soc. Discuss.* **28**, 168 (1959).
- <sup>36</sup>D. Eger, A. Many, and Y. Goldstein, *Surf. Sci.* **58**, 18 (1976).
- <sup>37</sup>D. Eger and Y. Goldstein, *Phys. Rev. B* **15**, (to be published).
- <sup>38</sup>Y. Goldstein and Y. Grinshpan, *Phys. Rev. Lett.* **39**, 953 (1977).
- <sup>39</sup>A. Many, Y. Goldstein, and N. B. Grover, *Semiconductor Surfaces* (North-Holland, Amsterdam, 1965), pp. 295 and 323.
- <sup>40</sup>D. C. Licciardello and D. J. Thouless, *Phys. Rev. Lett.* **35**, 1475 (1975); *J. Phys. C* **8**, 4157 (1975); *Surf. Sci.* **58**, 89 (1976).
- <sup>41</sup>J. R. Schrieffer, *Phys. Rev.* **97**, 641 (1955).
- <sup>42</sup>R. F. Greene, *Crit. Rev. Solid State Sci.* **4**, 477 (1974).
- <sup>43</sup>T. H. Di Stefano, *Appl. Phys. Lett.* **19**, 280 (1971).
- <sup>44</sup>R. Williams and M. H. Woods, *J. Appl. Phys.* **43**, 4142 (1972).
- <sup>45</sup>R. Williams and M. H. Woods, *Appl. Phys. Lett.* **22**, 458 (1973).